DALTON

Synthesis and characterization of alkoxo-oxygen-bridged copper(II) complexes having disc- and rod-like shapes†

Shingo Eguchia,[a] Takeshi Nozaki,[a] Hitoshi Miyasaka,[a] Naohide Matsumoto,*[,a] Hisashi Okawa,[a] Susumu Kohata[b] and Naomi Hoshino-Miyajima*[,c]

[a] *Department of Chemistry, Faculty of Science, Kyushu University, Hakozaki, Higashi-ku, Fukuoka 812, Japan*
[b] *Yatsushiro National College of Technology, Hirayamashinmachi 2627, Yatsushiro 866, Japan*
[c] *Department of Chemistry, Faculty of Science, Hokkaido University, Sapporo 060, Japan*

A series of copper(II) complexes with tridentate Schiff bases, obtained by the 1 : 1 condensation of a 4-(*p*-*n*-alkoxybenzoyloxy)salicylaldehyde and an aminoalcohol have been prepared and characterized, where the *n*-alkoxy group is *n*-propyloxy, *n*-butyloxy, *n*-hexyloxy, *n*-octyloxy, *n*-hexadecyloxy or *n*-octadecyloxy and the aminoalcohol is 2-aminoethanol, 3-aminopropanol, (*R*)- or (*S*)-2-amino-4-methylpentanol. The nineteen complexes thus synthesized can be classified into two groups, A and B; group A contain a 3-aminopropanol residue and B one of the remaining aminoalcohol residues. Group A members are reddish violet and almost diamagnetic, and it is deduced that these molecules are rod-like in shape and involve a binuclear Cu_2O_2 central core; group B are blue and paramagnetic, and likely to have a tetranuclear Cu_4O_4 central core of cubane-like structure and overall disc-like molecular shape. Polarized microscopic, differential scanning calorimetry, and heating X-ray diffractometry measurements were made to study the thermotropic mesomorphism. Polymorphic transitions have been characterized for representative complexes from groups A and B.

Liquid-crystalline materials containing metal ions (metallomesogens) have attracted much attention in recent years, because the combination of the properties of organic liquid crystals and of transition-metal ions can produce new materials exhibiting unique assembly structures, and optical, magnetic and electronic properties.[1] Organic liquid crystals can be divided into thermotropics and lyotropics. Thermotropics can be further sub-divided into calamitic and discotic, which are obtained with rod-like and disc-like molecules, respectively. Metal complexes show a remarkable variety of co-ordination geometries, so that co-ordination of liquid-crystalline compounds to metal ions can give a variety of molecular shapes. In addition to the versatility of the co-ordination geometry of mononuclear metal complexes, the arrangements of ligands at polynuclear metal sites can be useful to furnish exotic structures for the liquid crystalline phase.

In this paper, our attempts to produce liquid crystals with molecules of rod- and disc-like structures having polynuclear metal complex cores are reported. We selected copper(II) complexes with tridentate Schiff-base ligands formed by 1 : 1 condensation of 4-(*p*-*n*-alkoxybenzoyloxy)salicylaldehydes and aminoalcohols, based on the previous findings[2–9] and the following reasoning. (1) Mononuclear copper(II) complexes of Schiff bases formed from 4-(*p*-*n*-alkoxybenzoyloxy)salicylaldehyde and monoalkylamines have precedents which are liquid crystalline,[10,11] (2) copper(II) complexes with tridentate hydroxylated salicylaldimines possess either of two polynuclear chelate structures depending on the type of aminoalcohol, namely 3-(*N*-salicylideneamino)propanol forms an alkoxo-oxygen-bridged binuclear complex, while 2-(*N*-salicylideneamino)ethanol gives a tetranuclear cubane-like structure, and (3) when a *p*-*n*-alkoxybenzoyloxy group is introduced at the 4 position of the salicylidene moiety of these complexes, rod- and disc-like shapes are anticipated for the bi- and tetra-nuclear complexes, respectively. Fig. 1 shows the plausible structures for the last two species on the basis of X-ray analyses of the unsubstituted analogues.[9] One of the chancy elements is the arrangement of the substituents, particularly into the disc-like shape. There has been no example of metallomesogens of

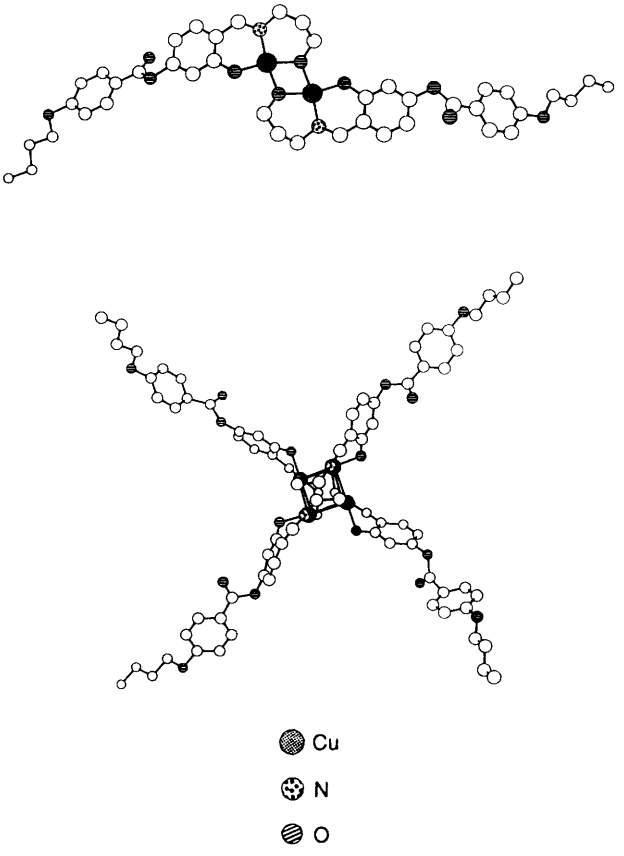

Fig. 1 Possible structures for binuclear complexes with a Cu_2O_2 core and tetranuclear complexes with a cubane Cu_4O_4 core, showing disk- and rod-like structures, respectively

† *Non-SI unit employed:* $\mu_B \approx 9.27 \times 10^{-24}$ J T^{-1}.

tetrahedral symmetry, but the present polynuclear species might be able to adopt conformations favouring anisotropic interactions.

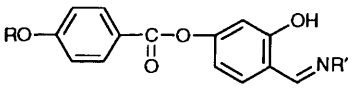

H_2L^n

A series of copper(II) complexes with tridentate Schiff bases H_2L^n obtained by 1:1 condensation of a 4-(*p*-*n*-alkoxybenzoyloxy)salicylaldehyde and an aminoalcohol have thus been prepared and characterized, where the aldehyde component carries an *n*-propyloxy, *n*-butyloxy, *n*-hexyloxy, *n*-octyloxy, *n*-hexadecyloxy or *n*-octadecyloxy end group (RO), and the aminoalcohol (H_2NR') is 2-aminoethanol, 3-aminopropanol or (*S*)- and (*R*)-2-amino-4-methylpentanol (leucinol) (see Table 1). The new complexes do not form the expected liquid-crystalline phases, but long-chain derivatives of both of the polynuclear types do exhibit precursor, highly disordered crystalline states.

Results and Discussion

Synthesis and characterization

The tridentate Schiff bases H_2L^n were easily prepared by mixing the component compounds in a methanol–chloroform mixture, which was then used for the synthesis of the copper(II) complex without isolating the base. The complexes were also readily synthesized by mixing the Schiff base, copper(II) acetate monohydrate, and triethylamine in 1:1:2 molar ratio in the same solvent. They are generally soluble in chloroform and insoluble in methanol, so that the recrystallization was carried out also from the chloroform–methanol mixture. Characterization data for the nineteen new complexes are given in Table 1.

The complexes containing a 3-aminopropanol residue **3a**–**3f** were obtained as reddish violet fine crystalline materials with a variable grey tint, while those containing a 2-aminoethanol **1a**–**1e**, (*S*)- or (*R*)-leucinol residue **2a'**, **2a**–**2f** were blue fine crystalline materials; **3** are less soluble in chloroform than the others and participate in a six-membered chelate ring with the aminoalcohol moiety, while the others have a five-membered chelate ring. The complexes can be classified into two groups A and B, exhibiting d–d band maxima at *ca.* 570 and *ca.* 620 nm, respectively, which are compatible with those of the related binuclear complex **4** (564 nm) and the cubane tetranuclear complex **5** (636 nm), of copper(II) with the condensation products of 3-ethoxymethylenepentane-2,4-dione and 3-aminopropanol and 2-aminoethanol, respectively.[2,3] The polynuclear structures of **4** and **5**, where the copper(II) ions assume four-co-ordinate square-planar [2] and five-co-ordinate square-pyramidal geometry,[3] respectively, have been confirmed by X-ray analysis. It can be concluded that the present group A and B complexes also assume square-planar and square-pyramidal co-ordination geometry, respectively.

Magnetic properties

The magnetic susceptibilities of the complexes were measured and the effective magnetic moments μ_{eff} per Cu at room temperature are given in Table 1. On the basis of these the complexes can be also classified into two groups and this classification is in accord with that on the basis of the electronic spectra. Group A complexes are almost diamagnetic, while group B exhibit normal effective magnetic moments around 1.7 μ_B per Cu. Plots of μ_{eff} *vs.* *T* are shown in Fig. 2 for **2e** and **3e** (R = $C_{16}H_{33}$), representing groups B and A, respectively.

The plot for complex **3e** is reproducible by the Bleaney–Bowers equation based on the spin Hamiltonian for a binuclear

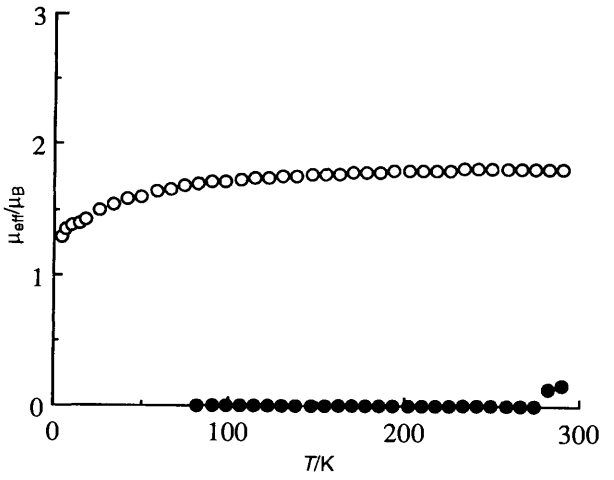

Fig. 2 Plots of μ_{eff} *vs.* *T* curves for complexes **2e** (○) and **3e** (●) showing that they are paramagnetic and nearly diamagnetic, respectively; μ_{eff} is the effective magnetic moment per copper atom

structure, $H = 2JS_1 \cdot S_2$. The best-fit parameter is $J = -450$ cm^{-1}, indicating a strong antiferromagnetic coupling between two copper(II) ions. The other group A complexes also exhibit very strong antiferromagnetic coupling parameters and consequently are almost diamagnetic, comparable to those of the related alkoxo-oxygen-bridged binuclear copper(II) complexes derived from 3-aminopropanol.[2–8]

On the other hand, the μ_{eff} of complex **1e** (R = $C_{16}H_{33}$) remains constant (*ca.* 1.66 μ_B from 290 K to 80 K) and then decreases to 1.27 μ_B at 4.5 K, where the magnetic susceptibility obeys the Curie–Weiss law $[1/\chi_A = C(T - \theta)]$ with a negative Weiss constant of −4.4 K, indicating the operation of a weak antiferromagnetic interaction. The μ_{eff} *vs.* *T* behaviours of the other group B complexes measured at 80–300 K obey the Curie–Weiss law, with Weiss constants θ varying from −7.2 to a +28.0 K depending on the chain length (Table 1). It is noteworthy that complexes with longer alkoxy chains (16 and 18) have negative Weiss constants and those with shorter chains have positive ones. A number of studies of copper(II) complexes with aminoalcohol residues have been carried out, and the correlations among nuclearity, chelate ring size, and magnetic properties have been established.[2–9] The present group B complexes with either positive or negative Weiss constants are expected to assume the tetranuclear Cu_4O_4 core structure, although differences in the relative bond distances or distortion in the Cu_4O_4 core may lead to a different mechanism of magnetic coupling.

FAB mass spectra

We attempted to grow single crystals suitable for X-ray analysis to confirm the polynuclear structures and the detailed structure. Single crystals of complexes **1b** and **2b** (R = Bu) were obtained by the diffusion method in 2-methylpropan-1-ol and chloroform. The needle crystals thus obtained, however, easily lose the crystal solvent and the X-ray diffraction intensities of the crystal encapsulated in a glass capillary were very weak. Owing to the poor quality of the crystals and the weak reflection data it was not possible to obtain structural information by X-ray analysis. Instead, the FAB mass spectra of **2c** and **3c** (R = C_6H_{13}) were recorded in *m*-nitrobenzyl alcohol, and revealed their nuclearities. Molecular-ion peaks corresponding to binuclear $[(CuL^{16})_2]^+$ (m/z = 921.7) and tetranuclear $[(CuL^9)_4]^+$ (m/z = 2012.2) cationic species were observed.

Introduction of an optically active group

The optically active aminoalcohols, (*S*)- and (*R*)-leucinol [$Pr^iCH_2C^*H(NH_2)CH_2OH$] were used in this study because

chiral liquid-crystalline phases have attracted great interest due to their potential ferroelectric and non-linear optical properties.[1,2] The circular dichroism spectra for **2e** (*R*) and **2e'** (*S*) (R = $C_{16}H_{33}$) (*ca.* 10^{-3} mol dm^{-3}) in chloroform are shown in Fig. 3, showing the antisymmetrical spectral pattern between the two complexes. This result indicates that the optical activity of the ligands simply reflects that of the complexes. It is stressed that an optically active moiety can be easily introduced into the metal complexes in this system.

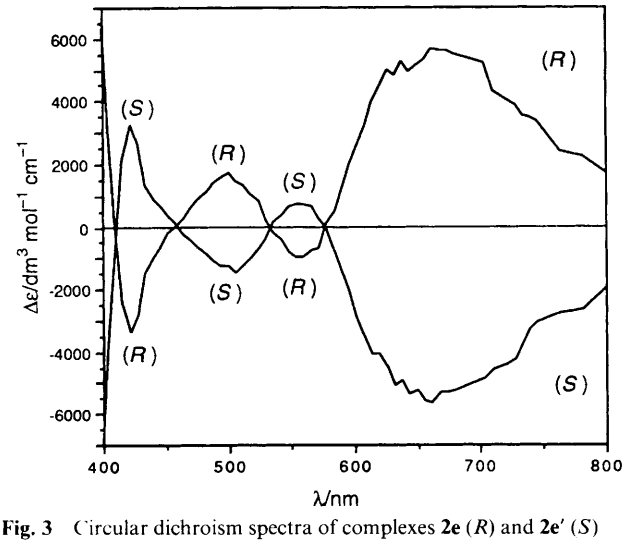

Fig. 3 Circular dichroism spectra of complexes **2e** (*R*) and **2e'** (*S*)

Thermal properities

The phase transition and optical characteristics of heated samples have been investigated for selected compounds in the hope of detecting thermotropic mesomorphism. Routine measurements of the melting points revealed that none of complexes **1** and lower homologues of **3** melts before decomposing. On the other hand, long-chain derivatives of the latter (16 and 18) and complexes **2** showed distinct melting points (Table 1). These materials also exhibited considerable 'softening' prior to clear melting, which gave the appearance of a mosaic or sandy texture under a polarizing microscope in some cases, leaving the possibility that these high-temperature phases might be mesophases, albeit relatively ordered. Unfortunately no monotropic mesophase transition was observable, due to thermal decomposition in the molten state.

Results of DSC measurements for selected complexes are summarized in Table 2. The major endothermic peaks of **2d** (R = C_8H_{17}) at 173 and 182 °C were separated by an exothermic drift of the thermogram, which implies double melting behaviour. Unfortunately an attempt to obtain a single-phase specimen by thermal annealing at 160 °C for half an hour led to sample degradation. The long-chain homologues, **2e** (R = $C_{16}H_{33}$) and **2f** (R = $C_{18}H_{37}$), display very large endothermic peaks around 100 °C, and then another peak

Table 1 Elemental analyses, absorption spectral, and magnetic data for the new complexes

	H_2L^n		Analysis (%)[a]				d–d band λ_{max}/nm	M.p. or decomp.	μ_{eff} per Cu/μ_B[b]
Complex	R	R'	C	H	N	Metal	(ε/dm^3 mol^{-1} cm^{-1})	point/°C	(θ/K)
1a [CuL^1]·0.25H_2O	Pr	C_2H_4OH	55.65	4.70	3.50	15.70	614	215–220	1.86
			(55.75)	(4.80)	(3.40)	(15.50)	(160)	(decomp.)	(+9.4)
1b [CuL^2]·0.5H_2O	Bu	C_2H_4OH	55.85	4.90	3.45	15.00	616	205–210	1.89
			(56.15)	(5.20)	(3.25)	(14.85)	(170)	(decomp.)	(+6.5)
1c [CuL^3]·0.5MeOH	C_6H_{13}	C_2H_4OH	58.20	5.65	3.05	13.65	611	213–218	1.87
			(58.35)	(5.90)	(3.05)	(13.70)	(166)	(decomp.)	(+22.6)
1d [CuL^4]	C_8H_{17}	C_2H_4OH	60.45	6.15	2.95	13.50	617	221–223	1.84
			(60.70)	(6.15)	(2.95)	(13.40)	(151)	(decomp.)	(+23.3)
1e [CuL^5]	$C_{16}H_{33}$	C_2H_4OH	65.50	7.70	2.40	10.75	617	215–220	1.66
			(65.45)	(7.70)	(2.40)	(10.80)	(178)	(decomp.)	(−4.4)
2a [CuL^6]	Pr	*R*-$C_5H_{12}OH$	59.55	5.95	3.00	14.10	620	231–234	
			(59.90)	(5.90)	(3.05)	(13.80)	(144)	(decomp.)	
2a' [CuL^7]	Pr	*S*-$C_5H_{12}OH$	59.75	6.00	3.15	14.05	618	232–234	1.84
			(59.90)	(5.90)	(3.05)	(13.80)	(154)	(decomp.)	(+28.0)
2b [CuL^8]	Bu	*R*-$C_5H_{12}OH$	60.70	6.10	3.00	13.45	614	223–227	1.80
			(60.70)	(6.15)	(2.95)	(13.40)	(159)	(decomp.)	(+27.7)
2c [CuL^9]	C_6H_{13}	*R*-$C_5H_{12}OH$	62.05	6.55	2.70	12.60	620	205, 210	1.81
			(62.05)	(6.60)	(2.80)	(12.65)	(167)		(+26.4)
2d [CuL^{10}]	C_8H_{17}	*R*-$C_5H_{12}OH$	63.20	7.00	2.65	11.85	614	175, 188	1.82
			(63.30)	(7.00)	(2.65)	(11.95)	(166)		(+26.4)
2e [CuL^{11}]·0.5$CHCl_3$	$C_{16}H_{33}$	*R*-$C_5H_{12}OH$	62.15	7.60	2.00	9.25	615	173	1.73
			(62.35)	(7.65)	(2.00)	(9.05)	(174)		(−16.7)
2e' [CuL^{12}]·0.5$CHCl_3$	$C_{16}H_{33}$	*S*-$C_5H_{12}OH$	62.30	7.60	2.15	8.55	615	173	
			(62.35)	(7.65)	(2.00)	(9.05)	(174)		
2f [CuL^{13}]·0.5$CHCl_3$	$C_{18}H_{37}$	*R*-$C_5H_{12}CH$	63.10	7.90	1.90	8.45	615	173	1.64
			(63.25)	(7.95)	(1.90)	(8.70)	(159)		(−7.2)
3a [CuL^{14}]·0.5MeOH	Pr	C_3H_6OH	56.45	5.05	3.35	14.80	572	257–262	0.69
			(56.60)	(5.35)	(3.20)	(14.60)	(135)	(decomp.)	
3b [CuL^{15}]·0.5H_2O	Bu	C_3H_6OH	56.90	5.25	3.30	14.65	573	263–265	0.51
			(57.05)	(5.45)	(3.15)	(14.40)	(147)	(decomp.)	
3c [CuL^{16}]·0.5MeOH	C_6H_{13}	C_3H_6OH	59.40	5.85	3.10	13.70	571	244–247	0.43
			(59.15)	(6.15)	(2.95)	(13.30)	(130)	(decomp.)	
3d [CuL^{17}]	C_8H_{17}	C_3H_6OH	61.60	6.35	2.75	13.05	574	243–245	0.48
			(61.40)	(6.40)	(2.85)	(13.00)	(128)	(decomp.)	
3e [CuL^{18}]·0.25H_2O	$C_{16}H_{33}$	C_3H_6OH	65.50	7.85	2.30	10.30	570	227	0.17
			(65.45)	(7.90)	(2.30)	(10.50)	(150)		
3f [CuL^{19}]·0.5MeOH	$C_{18}H_{37}$	C_3H_6OH	66.15	8.10	2.20	9.65	569	229	0.60
			(66.05)	(8.30)	(2.15)	(9.85)	(155)		

[a] Calculated values in parentheses. [b] At room temperature.

Table 2 Phase-transition temperatures (T/°C)[a] and enthalpies (ΔH/kJ mol^{-1})[b]

Compound		K_4	K_3	K_2	K_1(M)	I
2d	[CuL^{10}]		42	138	173,[c] 182	
			(26.4)	(7.5)	(61.6), (19.2)	
2e	[CuL^{11}]·0.5CHCl$_3$			98[d]	173	
				(181.6)[d]	(37.7)	
2f	[CuL^{13}]·0.5CHCl$_3$			100	173	
				(228.4)	(46.8)	
3e	[CuL^{18}]·0.25H$_2$O	75	112	153	227	
		(8.1)	(25.6)	(20.0)	(44.7)	
3f	[CuL^{19}]·0.5MeOH	81	116	148	229	
		(8.0)	(29.4)	(26.1)	(30.4)	

[a] The DSC peak temperatures recorded during the first heating scan with pristine solid samples are listed. Phase sequence and notations (K and I are for crystalline and isotropic liquid phases, and M for possible mesophase, respectively) are shown. Crystalline polymorphs are numbered only for designation from the highest-temperature phase down. [b] In parentheses. [c] Presumed to be melting of K_2 form. [d] Peak including the transition from K_3 to K_2 (see text).

commonly at 173 °C, which amounts only to one fifth of the preceding event. This thermogram pattern as well as the microscopic appearance of the sample above 100 °C suggests that the so-called K_1 phase may be liquid crystalline, but the magnitude of the isotropization enthalpy is quite large.

The binuclear complexes **3e** (R = $C_{16}H_{33}$) and **3f** (R = $C_{18}H_{37}$) showed multiple endothermic peaks, among which sharp transitions at 112 and 116 °C are associated with a change from reddish to greenish. The samples then gradually turned brown and softened on further heating. When the sample was cooled without melting the brown colour persisted with little sign of decomposition. The phase changes in these complexes are thus complicated, but again the final change in enthalpy upon clearing is rather large for a smectic.

Powder X-ray diffraction

X-Ray diffraction measurements were carried out for powdered samples of complexes **2e** and **3e** (R = $C_{16}H_{33}$) in order to determine the structures particularly of their K_1 phases. Selected diffraction data for each phase are reproduced in Figs. 4 and 5. The lowest-angle reflections are off-scale in these figures, and the corresponding peak distances are plotted against temperature in Fig. 6.

These low-angle reflections are related more to the longest molecular dimension, and the change in the longest periodicity, d_{max}, would reflect that in the ordering along this direction. It was found to serve as a useful probe for the phase transition events. Inspection of Fig. 6 reveals that the value of d_{max} jumps by as much as 8.1 Å upon the K_2 to K_1 transition for complex **2e**. The experiment also revealed that the material undergoes another transition from the room-temperature phase (K_3) to the K_2 phase at around 70 °C. This corresponds to the onset temperature for the large DSC endotherm peak at 98 °C and these transitions are not resolved by the thermal analysis. Neither of the reverse transitions from K_1 or K_2 was observed during cooling runs, which suggests that these phase changes involve desolvation. As Fig. 4 shows, a rather drastic change occurs in the medium-angle region of the diffraction pattern at the K_3 to K_2 transition, and another notable change is seen in the high-angle region at the K_2 to K_1 transition. Sharp reflections are no longer observed beyond 2θ = 17° and diffuse scattering is maximized at the corresponding distance of d = 4.6 Å. The K_1 phase of **2e** is perhaps best described as a conformationally disordered crystal, in which the central chelate cores are still three-dimensionally ordered while the alkyl tails have melted and lengthened with an increased proportion of *trans* conformations.

A discontinuous change of 4.5 Å in d_{max} takes place at the K_3 to K_2 transition in the case of complex **3e**. The changes associated with the other two transitions are small, or more or less continuous. The reverse transition K_1 to K_2 was

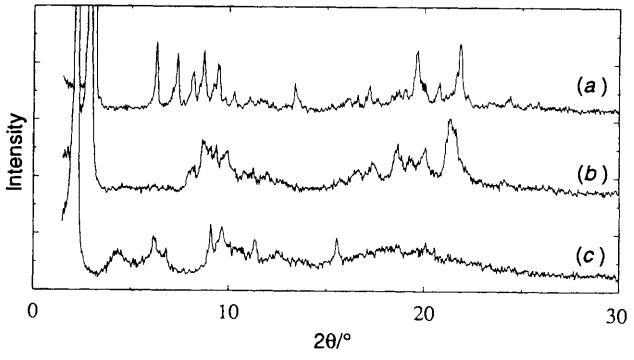

Fig. 4 Powder X-ray diffractograms for complex **2e** at (*a*) 55, (*b*) 83 and (*c*) 153 °C

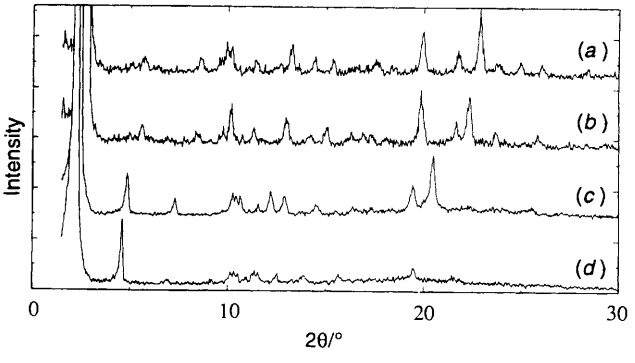

Fig. 5 Powder X-ray diffractograms for complex **3e** at (*a*) 50, (*b*) 90, (*c*) 122 and (*d*) 185 °C

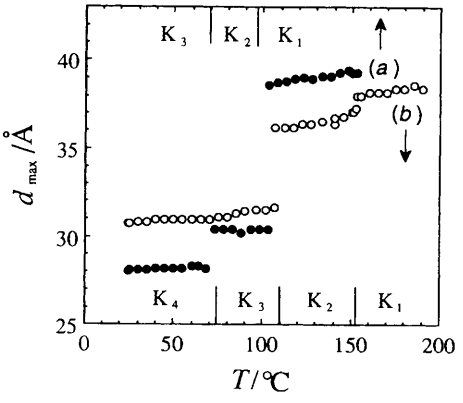

Fig. 6 Changes with temperature in the longest periodicity in the structures of complexes **2e** (*a*) and **3e** (*b*)

confirmed by the X-ray measurements, but the K_2 phase did not relax to a K_4 phase even after standing for 5 d at room

temperature. It is speculated that here again the K_3 to K_2 transition involves loss of solvent. Fig. 5 shows that the diffraction pattern differs little between the K_4 and K_3 phases, the major lamellar structure becomes distinctive in the K_2 phase, and finally the pattern appears nearly one-dimensional with the high-angle reflections largely diminished in the K_1 phase.

The 'residual' reflections are extracted for the K_1 phases and listed in Table 3. It was not possible to fit the pattern for complex **2e** by the two-dimensional lattices known for discotic liquid crystals of Dh or Dr[13] type. A tentative fit has been made based on a three-dimensional monoclinic unit cell and a model in space group $P2_1$ constitutes a molecular unit elongated along the *a* axis. The parameter $a = 43$ Å is very small compared to the molecular span. The R = Bu analogue of this complex depicted in Fig. 1, for instance, has a diagonal length of 42 Å. Therefore, it is speculated that the molten alkyl tails fill the space to form an overall elliptical shape. In the case of complex **3e** the fact that a number of weak but detectable reflections remain as listed in Table 3 indicates that it is more likely to be crystalline. A tentative fit to a three-dimensional monoclinic cell of space group $P2_1/c$, to which the crystal smectic H phase belongs, is also shown. The cell parameter $a = 42$ Å was hinted at by the data obtained for the liquid state, but this is again considerably smaller than the full molecular length. The R = Bu homologue of this complex (Fig. 1) is 38 Å long end-to-end. An interdigitated layer structure along the molecular long axis is an alternative explanation in this case since the diffuse scattering by the molten alkyl chains is relatively weak [Fig. 5(*d*)]. The model requires a dimeric constituent to give a reasonable value of the density. It can be imagined from the lattice parameters that, roughly speaking, the molecules stack along the *c* axis with a side-by-side array along the *b* axis. If molecular rotations would allow the *bc* plane to adopt hexagonal symmetry, a true liquid-crystalline, tilted smectic phase would be achieved. On the other hand, the monoclinic lattice of **2e** has a similar longitudinal dimension but a wider area of the *ab* face. In comparison to the binuclear counterpart, this dual system appears to be more flattened over this plane, but it seems to be still far from a discotic form.

Finally it may be worth referring to the X-ray diffraction profiles of the two complexes in their liquid states, from which information on the short-range ordering characteristics can be obtained. The tetranuclear complex **2e** exhibits a diffuse-scattering pattern with peak at around 13–14 and 5 Å, while the corresponding low-angle diffraction for the two-tail complex **3e** is relatively sharp and with a peak at 42 Å. Our scheme of constructing distinctively different units by the usage of different polynuclear complexes seems at least to work, but we are faced with the question of how to achieve the desired long-range orientational order. The small shape anisotropy, as deduced from the liquid state, of the 'disc-like' complex in the present design may not be sufficient for columnar (stacking) order to emerge. The substitution pattern around the cubane core is inherently of S_4 or C_2 symmetry and a new design would be necessary to enforce overall C_4 symmetry for the molecule with the large shape anisotropy. We are currently investigating new analogues, particularly of the leucinol complex derivatives, in which heavier alkoxy substitution might lead to enhanced van der Waals stacking interaction.[14]

Table 3 X-Ray diffraction data for the K_1 phases of complexes **2e** and **3e**

2e[a]			**3e**[b]		
d_{obs}/Å	d_{calc}/Å	Index	d_{obs}/Å	d_{calc}/Å	Index
39.06	39.06	100	38.05	38.06	100
20.0(br)	19.53	200	19.03	19.03	200
14.24	14.28	110	12.60	12.69	300
12.95	13.02	300	9.54	9.51	400
9.69	9.66	$11\bar{1}$	8.67	8.66	$20\bar{2}$
9.21	9.18	011	8.53	8.49	$30\bar{2}$
7.77	7.67	020	8.39	8.40	$10\bar{2}$
7.0 (br)	7.14	220	8.01	7.99	$11\bar{1}$
5.70	5.73	002	7.78	7.80	011
4.76w	4.74	$12\bar{2}$	7.61	7.61	500
4.41w	4.40	122	7.03	7.08	102
			6.33	6.33	202
			5.60	5.65	302
			4.52	4.50	020
			4.10	4.07	420

[a] Data at 150 °C. $a = 42.69$, $b = 15.34$, $c = 12.53$ Å, $\beta = 113.8°$; density of 1.14 g cm^{-3} obtained by assuming space group $P2_1$ and $Z = 2$. [b] Data at 170 °C. $a = 42.20$, $b = 9.00$, $c = 17.33$ Å, $\beta = 115.6°$; density of 1.33 g cm^{-3} obtained by assuming space group $P2_1/c$ and $Z = 4$.

Experimental

Materials

All chemicals and solvents used for the synthesis were of reagent grade. 4-(*p*-*n*-Alkoxybenzoyloxy)salicylaldehydes were prepared by literature methods,[15–17] the tridentate Schiff bases by mixing them and an aminoalcohol in 1:1 mole ratio in chloroform–methanol, and finally the copper(II) complexes by simply adding the starting copper salt to this solution. Two examples are described.

Complex 3e. To a solution of 4-(*p*-*n*-hexadecyloxybenzoyloxy)salicylaldehyde (0.47 g, 1 mmol) in chloroform (20 cm^3) and methanol (10 cm^3) was added a solution of 3-aminopropanol (0.06 g, 1 mmol) in methanol (5 cm^3). To the resulting yellow solution was added triethylamine (200 mg, 2 mmol) and then a solution of copper(II) acetate monohydrate (200 mg, 1 mmol) in methanol (20 cm^3). After stirring for several hours at room temperature, a reddish brown precipitate was collected by suction filtration, washed with methanol, and dried *in vacuo*. The crude sample was recrystallized from a mixture of chloroform and methanol. The other copper(II) complexes containing 3-aminopropanol were prepared similarly as reddish violet fine crystalline materials.

Complex 1e. This complex was prepared as above, but the solid which precipitated was blue. It was collected by suction filtration, washed with methanol, and dried *in vacuo*. The crude sample was recrystallized from a mixture of chloroform and methanol. The other copper(II) complexes containing 2-aminoethanol, (*S*)- and (*R*)-leucinol were prepared similarly as blue fine crystalline materials.

Physical measurements

Elemental analyses (C, H and N) were obtained at the Elemental Analysis Service Center of Kyushu University. Copper was analysed on a Shimadzu AA-680 atomic absorption/flame emission spectrophotometer. Melting points were recorded on a Yanagimoto apparatus and not corrected. Infrared spectra were recorded on a JASCO IR-810 spectrophotometer on KBr discs. Magnetic susceptibility measurements on powder samples were carried out with a HOXAN HSM-D SQUID susceptometer in the temperature range 4.4–80 K and a Faraday balance in the range 80–300 K.[18] The diamagnetism of the complex was estimated from Pascal's constants. The effective magnetic moments were calculated by the equation $\mu_{eff} = 2.828(\chi_A T)^{\frac{1}{2}}$, where χ_A is the magnetic susceptibility per copper(II) atom. The FAB (fast atom bombardment) mass spectra were recorded on a JMS-SX/SX102A Tandem mass spectrometer using *m*-nitrobenzyl alcohol as solvent, electronic absorption spectra on a Shimadzu

MPS-2000 multipurpose recording spectrophotometer and circular dichroism spectra of *ca.* 2 mmol dm^{-3} solutions on a JASCO J-600C instrument in chloroform. Differential scanning calorimetry (DSC) was carried out with a Rigaku Denki DSC TAS-200 apparatus. The sample temperature was varied between room temperature and several degrees higher than the melting point at a constant heating rate of 5 °C min^{-1}. The sensitivity of the instrument was 0.25 mcal s^{-1} (cal = 4.184 J) and α-Al_2O_3 was used as reference sample. The sample was packed into an aluminium pan and sealed. Mesomorphic phase-transition behaviours were examined by a Nikon OPTIPHOTO-POL polarizing microscope equipped with a Mettler FP82HT hot stage and a Mettler FP 90 temperature-control apparatus. Powder X-ray diffraction measurements were carried out at ambient and elevated temperatures using a Rigaku RAD-C diffractometer system equipped with a temperature-controlled furnace. The sample was maintained within ±0.1 °C of the set temperature.

References

1 S. A. Hudson and P. M. Maitlis, *Chem. Rev.*, 1993, **93**, 861, A.-M. G-Godquin and P. M. Maitlis, *Angew. Chem., Int. Ed. Engl.*, 1991, **30**, 375; P. Espinet, M. A. Esteruelas, L. A. Oro, J. L. Serrano and E. Sola, *Coord. Chem. Rev.*, 1992, **117**, 215; D. W. Bruce, *J. Chem. Soc., Dalton Trans.*, 1993, 2983.

2 N. Matsumoto, T. Tsutsumi, A. Ohyoshi and H. Okawa, *Bull. Chem. Soc. Jpn.*, 1983, **56**, 1388.

3 N. Matsumoto, T. Kondo, M. Kodera, H. Okawa and S. Kida, *Bull. Chem. Soc. Jpn.*, 1989, **62**, 4041.

4 J. A. Bertrand and J. A. Kelley, *Inorg. Chim. Acta*, 1970, **4**, 203.

5 R. Mergehenn, W. Hasse and R. Allmann, *Acta Crystallogr., Sect. B*, 1975, **31**, 1847.

6 E. D. Estes and D. J. Hodgeson, *Inorg. Chem.*, 1975, **14**, 334.

7 N. Matsumoto, I. Ueda, Y. Nishida and S. Kida, *Bull. Chem. Soc. Jpn.*, 1976, **49**, 1308.

8 Y. Nishida and S. Kida, *J. Inorg. Nucl. Chem.*, 1976, **38**, 451.

9 C. J. Cairns and D. H. Busch, *Coord. Chem. Rev.*, 1986, **69**, 1.

10 N. Hoshino, H. Murakami, Y. Matsunaga, T. Inabe and Y. Maruyama, *Inorg. Chem.*, 1990, **29**, 1177.

11 N. Hoshino, A. Kodama, T. Shibuya, Y. Matsunaga and S. Miyajima, *Inorg. Chem.*, 1991, **30**, 3091.

12 M. Marcos, J. L. Serrano, T. Sierra and M. J. Gimenez, *Angew. Chem., Int. Ed. Engl.*, 1992, **31**, 1471; C. F. van Nostrum, A. W. Bosman, G. H. Gelinck, S. J. Picken, P. G. Schouten, J. M. Warman, A.-J. Schouten and R. J. M. Nolte, *J. Chem. Soc., Chem. Commun.*, **1993**, 1120.

13 K. Ohta, O. Takenaka, H. Hasebe, Y. Morizumi, T. Fujimoto and I. Yamamoto, *Mol. Cryst. Liq. Cryst.*, 1991, **195**, 135.

14 H. Zheng and T. M. Swager, *J. Am. Chem. Soc.*, 1994, **116**, 761.

15 M. E. Neubert, S. J. Laskos, jun., L. J. Maurer, L. T. Carlino and J. P. Ferrato, *Mol. Cryst. Liq. Cryst.*, 1978, **44**, 197.

16 M. Ikeda and T. Hatakeyama, *Mol. Cryst. Liq. Cryst.*, 1976, **33**, 201.

17 A. Hassner and V. Alexanian, *Tetrahedron Lett.*, 1978, **46**, 4475.

18 E. A. Boudreaux and L. N. Mulay, *Theory and Applications of Molecular Paramagnetism*, Wiley, New York, 1976, p. 491.

Received 15*th September* 1995; *Paper* 5/06104K